

Interaction carboxylic acids – light in an aqueous medium and their implication in the elimination of carbamazepine

A. Boudib*, N. Debbache*, N. Seraghni, B.A. Dekkiche, T. Sehili

Laboratoire des Sciences et Technologies de l'Environnement (LSTE), Faculté de Chimie, Université des Frères Mentouri, Constantine 1, Algérie, emails: boudib.asma@umc.edu.dz (A. Boudib), nadradebbache@yahoo.fr (N. Debbache), wassila.seraghni@umc.edu.dz (N. Seraghni), anfel.dekkiche@umc.edu.dz (B.A. Dekkiche), tsehili@yahoo.fr (T. Sehili)

Received 11 June 2021; Accepted 3 October 2021

ABSTRACT

In the present study, we have investigated the photolysis of aliphatic and aromatic carboxylic organic acids (malic, oxalic, iminodiacetic, salicylic and benzoic) under both blacklight lamps and solar light. The ability of these acids to produce hydroxyl radicals under UVA radiation was also examined. Several experiments have been conducted to establish a relationship between the nature of the organic acid and the efficiency of the production of these radicals by the Fenton reaction. The results of this study suggest that the generation of hydrogen peroxide was influenced by the irradiation wavelength, the initial concentration of the carboxylic acid, the pH and the nature of the acid. Carbamazepine (CBZ) degradation induced by organic acids/UV system in aqueous solution was tested and confirmed that photocatalytic efficiency is optimal when oxalic acid is used. CBZ mineralization was followed by total organic carbon (TOC) analyzer, the mineralization efficiency reaches 80% of TOC removal after 14 h of irradiation (CBZ/oxalate/UVA system). Upon solar irradiation, a complete CBZ disappearance takes place after 1 h in system oxalic acid/CBZ.

Keywords: Carbamazepine; Carboxylic acids; Fe(III)-salicylic complex; Hydrogen peroxide; Hydroxyl radicals

1. Introduction

Carboxylic acids have received considerable attention as one of the organic compounds generally present in dissolved form in the natural environment [1,2]. They are also considered as the most dominant classes of organic compounds found in the atmosphere in a variety of phases. Carboxylic acids are found in relatively high amounts in all of the environmental compartments (atmosphere, aquatic media and soil) [3,4]. Measurements of carboxylic acid concentrations in cloud waters have been performed in several studies [5–7]. They represent up to 10% of the dissolved organic carbon in clouds [7,8], and can significantly contribute to the acidity of atmospheric precipitations [6].

Water-soluble dicarboxylic acids may also be produced from photochemical and aqueous phase oxidation

of biogenic unsaturated fatty acids and volatile organic compounds such as isoprene emitted from the ocean surface [9,10]. These compounds are usually classified into two types of carboxylic acids: aromatic acids (A-Ar) and aliphatic acids (A-Ali). A-Ali is also divided into different classes: monoacids, diacids, polycarboxylic, and amino-polycarboxylic. They are also highly relevant pollutants because of their toxicity and low biodegradability [11].

Organic acids ($R-CO_2H$) represent a class of compounds abundant in natural waters able to form complexes with a variety of transition metals (including Fe(III)) [12,13]. Oxalic and glyoxylic acid appears to have a free tropospheric air chemical source. The hydroxyl radical (HO^\bullet) is considered the main oxidative species present in the atmospheric aqueous phase. As a function of photochemical conditions, cloud chemistry models between 10^{-14} and 10^{-12} M evaluate

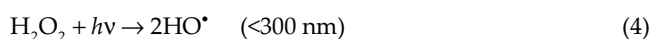
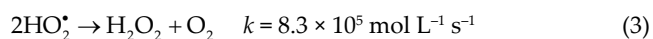
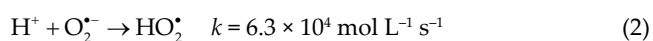
* Corresponding authors.

the maximal concentration (at noon) in natural water [14]. Silva et al. [15], Kuma et al. [16] reported that Fe(III) and citric acid or tartaric acid could form stable complexes. Moreover, these complexes have high photocatalytic activity [17,18].

Under light irradiation, photolysis of polycarboxylic acids leads to the formation of the oxidative species having an impact on the immediate environment. The literature indicates that the photolysis of polycarboxylic acids in the presence of dissolved oxygen could represent an important source of H₂O₂. The mechanism of the photolysis of organic was illustrated following sequences:

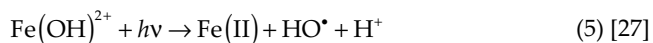


R: polycarboxylic acid or amino-polycarboxylic acid [19].



The photolysis of oxalic acid leads especially to the formation in situ of hydroxyl radical (HO[•]) [20].

Literature reports that the presence of carboxylic acids such as oxalic, citric or tartaric acids with Fe(III) and UVA radiation improves the water elimination rates of organics such as dyes [21,22], herbicides [15,23], pharmaceuticals [24,25], and other hydrocarbons [26]. The reason for this is due to the formation of ferric-carboxylate complexes that may be photolyzed to yield free radicals (4).



Fe(III)-photocatalysis under sunlight is low cost and has been employed for the treatment of organic pollutants since the 1990s. Many studies have recognized that the photoexcitation of Fe(III)-carboxylate complexes in an aqueous medium induces the transfer of electrons from the ligand to the central metal ion (ligand to metal charge transfer, LMCT). This transfer results in a reduction of Fe³⁺ to Fe²⁺, formation of the hydroxyl radical (HO[•]), and oxidation of the ligand [28,29].

During the anterior work on the complexes, the tests were carried out on the acids of the corresponding complexes and the results showed an activity of these acids [30,31]. The mechanism of carbamazepine degradation has been investigated by many authors in many oxidative treatment processes, they reported that in these processes there is a formation of hydroxyl radicals [32–35]. The determination of H₂O₂ and the disappearance of the acid will guide us in the understanding of the mechanism of the photolysis of these acids.

The present work, therefore, was to determine the formation of HO[•] at different carboxylic acids, the fate of pollutants in the aquatic environment in the presence of light and polycarboxylic acid for the photodegradation process

of carbamazepine catalyzed by carboxylic acids and the reaction kinetics were investigated under irradiation with different light sources.

2. Experimental section

2.1. Reagents

DL-malic acid (99%) biochem, salicylic acid (98%), benzoic acid (100.2%), oxalic acid (≥99%), sulfuric acid (97%), benzene (99.7%), HClO₄ (35.7%) and NaOH (98%) were supplied by VWR Prolabo. Iminodiacetic acid (>98%) Alfa Aesar. TiCl₄ (98%) was obtained from Flucka. Carbamazepine (CBZ) (99%) was purchased from the pharmaceutical industry. Using all products without purification because was the analytical grade. Using the ultrapure water supplied by a Milli-Q device (Millipore, Bedford, MA, USA) with resistivity (R = 18 MΩ cm) for preparing the solutions. The solutions were dissolved in ultrapure water.

2.2. Irradiation device

The use of a device fitted with a Pyrex tube in the center of a stainless steel cylinder. The lamp as the light source is a medium pressure mercury vapor lamp (Philips HPW 125), the emission of which, filtered by a black globe, is mainly at 365 nm with irradiation intensity $I = 1.97 \text{ mW cm}^{-2}$. The infrared component of the lamp emission is fully absorbed by the water surrounding the reactor. The solutions were cooled by water circulation and kept under agitation during the experiment (Fig. 1).

The solutions were irradiated in a cylindrical quartz reactor, surrounded by three low-pressure mercury lamps with maximum emissions at 254 nm (Fig. 2).

The solutions were irradiated under natural sunlight in a cylindrical Pyrex reactor in Constantine (Algeria), latitude 36°20'N, longitude 6°37'E. The radiometer type VLX 3W was used to measure light intensity equal to 2.56 mW cm⁻².

2.3. Analysis of the reaction products

The spectrophotometer "Thermo Scientific" controlled by software "Thermo Insight" was used to record the absorbance spectra and quantify the concentration of H₂O₂ formed. The complexometric method with titanium tetrachloride (TiCl₄) was used to determine the amount of H₂O₂ formed during the reaction. The molar absorption coefficient 742 M⁻¹ cm⁻¹ was measured at 410 nm [36].

Hydroxylation of benzene (7 mM) by HO[•] to produce phenol, using to detect HO[•] generated in the irradiated carboxylic acids, with $k_{(HO^{\bullet} + benzene)} \approx 7.8 \cdot 10^9 \text{ L mol}^{-1} \text{ s}^{-1}$ [37].

The concentration of CBZ was analyzed by high-performance liquid chromatography, equipped with a photodiode-array detector (Shimadzu SPD-20A) and a SUPELCO HC-C18 column (5 μm, 250 mm × 4.6 mm). The mobile phase was constituted by a mixture of acetonitrile (50%) and water (50%) containing 0.1% acetic acid with a flow rate of 0.5 mL min⁻¹. The detector wavelength was set at 286 nm.

Total organic carbon (TOC) analyzer (Teledyne Tekmar Torch TOC) was used to measure the mineralization degree for CBZ degradation.

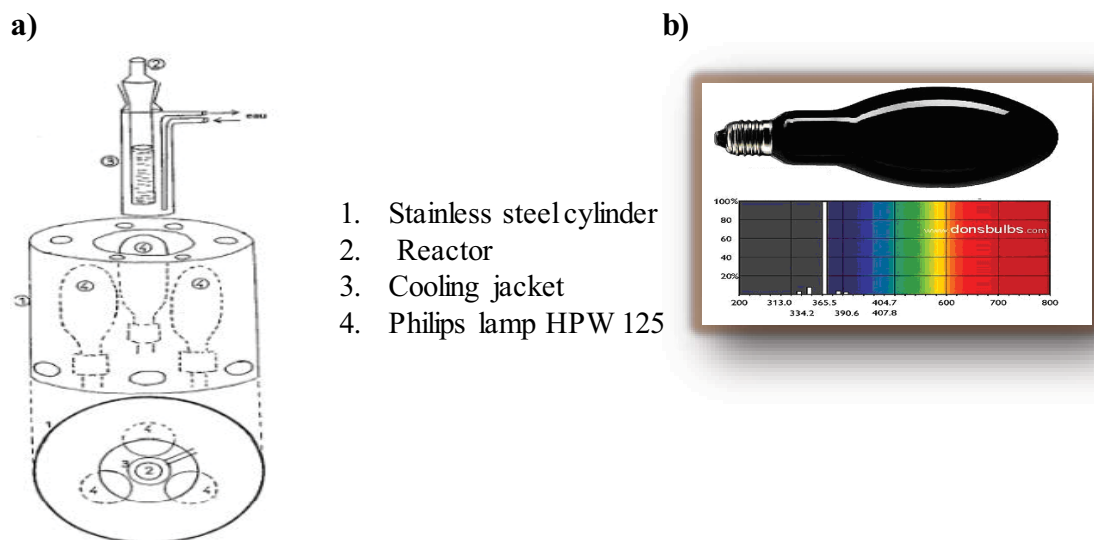


Fig. 1. (a) Monochromatic irradiation device at 365 nm and (b) emission spectrum of a lamp emitting at 365 nm.

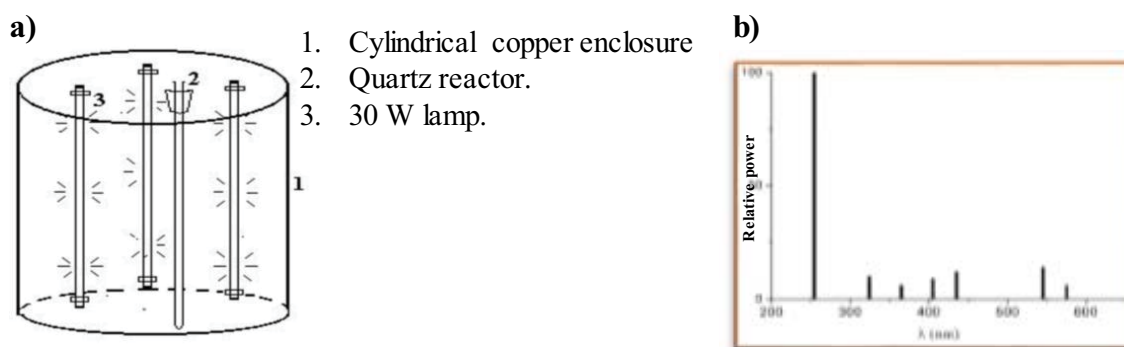


Fig. 2. (a) Monochromatic irradiation device at 254 nm and (b) emission spectrum of a lamp emitting at 254 nm.

3. Results and discussion

3.1. Properties of the carboxylic acids

Many references have reported the physical and chemical properties of carboxylic acids (SA, BE, MA, OX, IDA); the basic properties of these carboxylic acids were reviewed. Table 1 lists the acid properties.

3.2. Stability of acids

In the dark and at room temperature, an aqueous solution containing carboxylic acids (SA, BE, MA, OX, IDA concentration) for one week shows that carboxylic acids are stable in an aqueous solution.

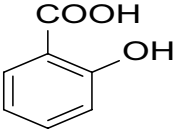
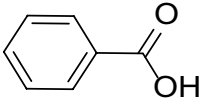
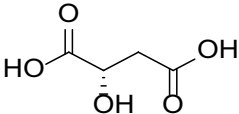
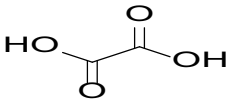
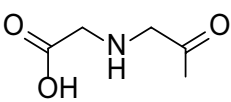
3.3. Photolysis of carboxylic acids

The concentration of carboxylic acids was kept constant at 5 mM, their photolysis up to 365 nm, provides an exciting state acid that underwent a further decomposition with the formation of HO^\bullet , $\text{O}_2^{\bullet-}$ and HO_2^\bullet as reported by Guo et al. [38]. We monitored these changes by spectrophotometry and quantified species formation by chemical methods.

3.3.1. Photolysis at 365 nm

The evolution UV-visible absorption spectrum of salicylic acid (SA) (5 mM) solution during irradiation at 365 nm is reported in Fig. 3a. No significant difference among the spectra at different times was observed. Indeed, a slight increase in absorbance in the 280–300 nm regions was reported in the insert (Fig. 3a). What's more, the benzoic acid (BE) evolution spectrum during irradiation reported in (Fig. 3b) has the same shape. The UV-visible absorption spectrum of malic acid (MA) during irradiation reported in Fig. 3c shows different variations located at region 210–240 nm. Indeed, their spectrum shows a very weak spectral evolution, namely a slight increase in absorbance (0.5) after 5 h. Moreover, three isosbestic points are present and localized at ($\lambda = 220$ nm in $t = 3$ h, $\lambda = 226$ nm in $t = 6$ h, $\lambda = 229$ nm in $t = 7$ h) point out the photolysis of the MA acid under irradiation at 365 nm. For the oxalic acid (OX), the UV-visible absorption spectrum during irradiation reported in Fig. 3d shows also a slight variation positioned at 225 nm. This reflects a transformation when organic acid was photolyzed at 365 nm. The UV-visible absorption spectrum of iminodiacetic acid (IDA) during

Table 1
Spectroscopy data on acids: structure, wavelengths of maximum absorption, molar absorption coefficients, solubility and pKa

Name	Structure	λ_{abs} (nm)	ϵ ($\text{M}^{-1} \text{cm}^{-1}$)	Solubility (g L^{-1})	pKa
SA		232 297	3,587	2.24	2.53 13.3
BE		272 229	9,267	2.9	4.9
MA		–	125.4	558	3.2 5.3
OX		–	166.86	220	1.27 4.35
IDA		–	42.02	42	2.4 9.7

(–) UV-Visible spectra of MA, OX, IDA acids absorb from 200 to 300 nm. No bands were detected.

irradiation is reported in Fig. 3e, the evolution is also located at 225 nm.

The disappearance of all organic acids was followed and it turns out that oxalic acid has the greatest disappearance (Fig. 4).

In order to elucidate the formation of H_2O_2 , as shown in Eqs. (1) and (2), hydrogen peroxide was determined by the formation of a yellow complex with TiCl_4 . During irradiation of acid (5 mM) under UV light, the quantification of hydrogen peroxide generated illustrated in Fig. 5 gives evidence of a big correlation between photolysis of organic acids efficiency and the amount of H_2O_2 generated.

The oxalic acid that disappears the fastest, gives the largest amount of H_2O_2 . Table 2 illustrates this fate.

3.3.2. Effect of pH

The pH effect on the formation of H_2O_2 was also examined. A solution containing 5 mM of acids was adjusted by adding acid or base. The results reported in Table 3 illustrated this fact.

The percentage of the disappearance of the carboxylic acids studied as a function of the pH is small; indeed, the disappearance there is a change of the spectrum and the appearance of the isosbestic points. On the other hand, the formation of H_2O_2 shows that at:

- SA acid ($\text{pH} < 3$), the H_2SA species are the most predominant and at this range the amount of H_2O_2 generated is great with the acidity of the medium. However, at $3 < \text{pH} < 8$. The HAS^- species are the most predominant characterized by a large generation of H_2O_2 .

- BE acid ($\text{pH} < 4$), the HBE_{aq} species characterized by a large generation of H_2O_2 are the most predominant. At $\text{pH} > 4$, where the most dominant form BE^- , no formation of H_2O_2 .
- MA acid ($\text{pH} > 4$) the H_2MA and HMA^- species characterized by a large generation of H_2O_2 are the most predominant. However, at $\text{pH} = 4.3$, $\text{pH} = 6.76$, only HMA^- , MA^{2-} species are present respectively. The formation of H_2O_2 at these pH is outside the detection limits.
- IDA acid has different species at pH range ($\text{pH} < 4$), $\text{H}_3\text{IDA}/\text{HIDA}^-/\text{HIDA}^{2-}$ species are the most predominant, and when $\text{pH} > 4$, the only HIDA^{2-} species which exists at this pH. Where the most dominant form of all this species formation is outside the detection limits.
- OX acid ($\text{pH} = 2.35$), the H_2OX and HOX^- species characterized by a large generation of H_2O_2 are the most predominant. However, when the $\text{pH} = 3.15$. The only occurring species is HOX^- . At this pH, the formation is less important than that observed in the preceding case. At $\text{pH} = 6.46$, where the most dominant form is OX^{2-} formation of H_2O_2 is outside the detection limits. For the other acids, the amount of H_2O_2 is ten times less than that of OX acid.

Fig. 6 presents the speciation of the carboxylic acids as a function of their concentration. From data shown in Table 3 and by examining the speciation of each acid and the evaluation of the absorbance in the UV-Visible range the following conclusions can be drawn:

- Aromatic acids (this is the case of salicylic and benzoic acids) that have HA^- species characterized by a large generation of H_2O_2 are the most predominant.

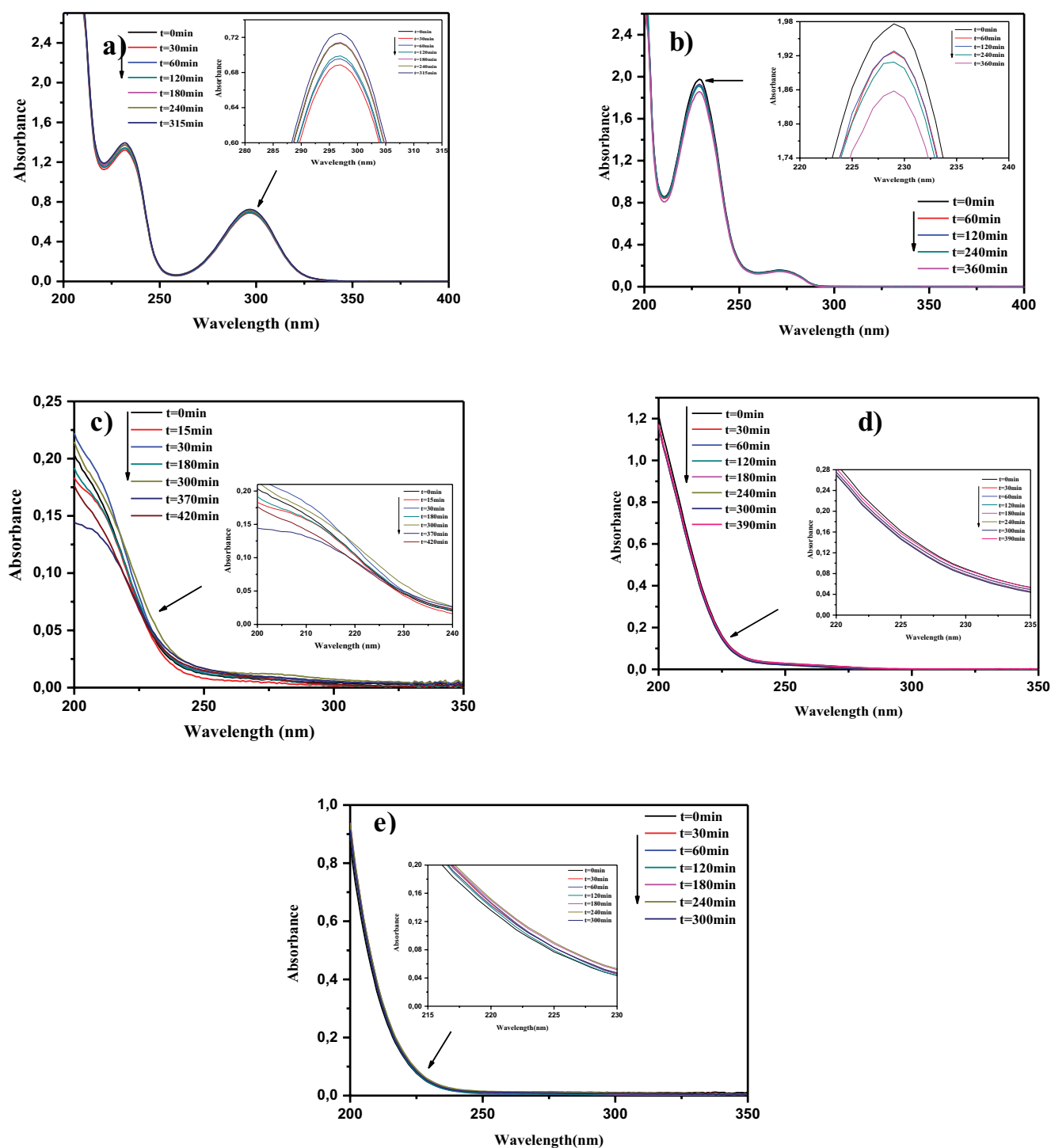
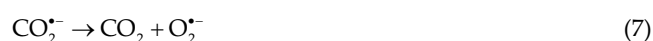


Fig. 3. Spectral evolution of acid (5 mM) upon irradiation at 365 nm as a function of irradiation time. Insert: zoom of spectral evolution of acid SA, BE, MA, OX, and IDA at wavelength 297, 229, 225, 230 and 225 nm, respectively. (a) SA: pH = 2.7, (b) BE: pH = 3.2, (c) MA: pH = 3.03, (d) OX: pH = 2.35 and (e) IDA: pH = 2.85.

- In case of oxalic acid, it is the quantum yield that determines its efficiency of H₂O₂ generation and is not directly related to the percentage of acid abatement, in fact, it depends on the reaction with O₂ and the consequence of O₂^{•-}, through reactions [20,39,40]:



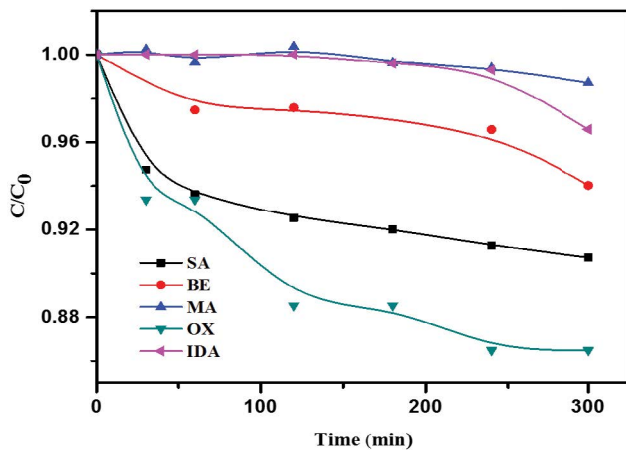


Fig. 4. Monitoring of disappearance of different acids upon irradiation at 365 nm as a function of irradiation time [acid] = 5 mM.

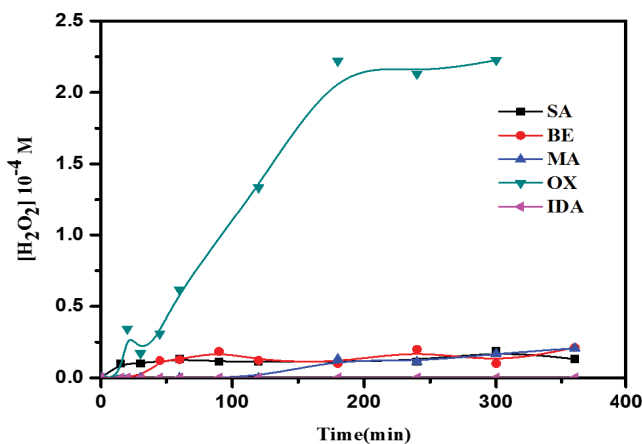
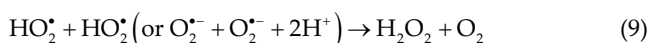


Fig. 5. Formation of H_2O_2 during the photolysis of different acids upon irradiation at 365 nm as a function of irradiation time [acid] = 5 mM.

Table 2
Abatement of carboxylic acids and H_2O_2 formation during their photolysis upon irradiation at 365 nm

Acids	SA	BE	MA	OX	IDA
% abatement	10	6	2	14	4
$[\text{H}_2\text{O}_2]_{\text{max}} \cdot 10^{-5}$ (M)	1.32	3.36	2.08	22.3	Lower than the detection limit
Time (h)	5	7	6	5	6



3.3.3. Effect of acids concentration

Experiments were carried out to investigate the initial concentration value effect on the photogeneration of H_2O_2 in the solution containing acids. The results shown in

Table 3
Abatement of acids and H_2O_2 formation during their photolysis as function of pH upon irradiation at 365 nm

Acids	pH	% abatement	$[\text{H}_2\text{O}_2]_{\text{max}} \cdot 10^{-5}$ (M)	Time/h
SA	2.7	10	1.32	5
	1.7	2	1.69	1
	7.3	15	3.2	7
BE	3.1	6	3.36	7
	2.5	4	2.26	6
	7.3	1	–	6
MA	3.03	2	2.08	6
	4.3	4	–	6
	6.76	1	–	6
OX	2.35	14	22.3	5
	3.15	26	15	5
	6.46	3	–	5
IDA	2.58	–*	–	6
	7.2	–*	–	6

(–): Lower than the detection limit;

(–): Appearance of isosbestic points and spectrum change.

Table 4 let us see that 5 mM seems to be the optimal initial concentration to produce a maximal amount of H_2O_2 .

3.3.4. Effect of irradiation wavelength

The photolysis of carboxylic acids (5 mM) under irradiation 254 nm, 365 nm and solar light are studied in order to establish the relationship between the acid photolysis and the H_2O_2 formation. The results summarized in Table 5, no relation was noticed between the nature of the acid and the irradiation intensity.

3.3.5. Hydroxyl radical quantification

The concentration of the HO^{\bullet} radicals generated by the photolysis of the carboxylic acids (SA, BE, MA, OX, IDA) was determined during the reaction. As shown in Fig. 7, after 7h of irradiation, the concentration of HO^{\bullet} generated in the solution containing the OX acid was $103.9 \mu\text{mol L}^{-1}$ at pH 2.35. These results indicated that under 365 nm irradiation, these acids were easily photolyzed and it provided the possibility for the formation of excited-state acids and further generated many kinds of radicals.

3.4. Phototransformation of carbamazepine induced by organic acids

To confirm the involvement of organic acid in the degradation of carbamazepine (CBZ) in the homogeneous system, the mixture (CBZ/OX; 0.01 mM/5 mM) was exposed to elimination using a UV lamp (365 nm). The following of CBZ disappearance as is reported in Fig. 8 showed that over 76% of the CBZ was transformed after 7 h in the system CBZ/OX/UV, due to the rapid photochemical reactions involving the OX/UV light system since the contribution of CBZ photolysis was insignificant. Otherwise, no

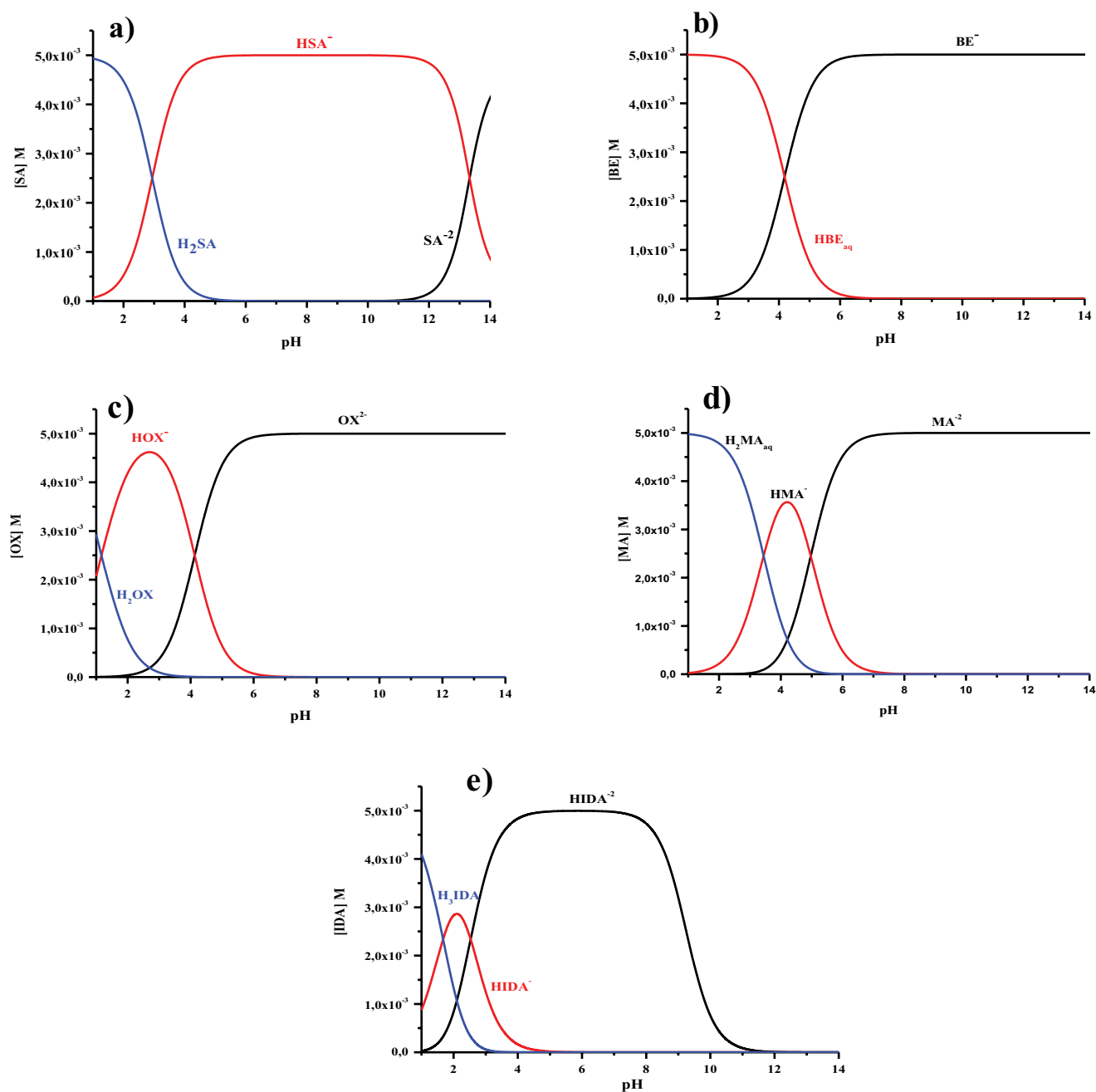


Fig. 6. Speciation of the acids calculated by the Hyperquad Simulation and Speciation (HYSS2009) as a function of the concentration of the acid.

interaction occurs between the components when this mixture ages in dark. Moreover, the positive effect of the OX can be attributed to the formation of the hydrogen peroxide produced *in-situ* by the direct photolysis of OX, giving rise to the formation of hydroxyl radicals which react rapidly and non-selectively on most of the organic compounds. Despite the low coefficient of absorption molar of H_2O_2 ($\epsilon_{254\text{ nm}} = 18.6 \text{ M}^{-1} \text{ cm}^{-1}$) to the wavelengths greater than 300 nm, the oxidation of CBZ has been observed in these conditions.

The concentration of H_2O_2 which can control HO^\bullet formation by photolysis reactions of oxalic acid was monitored, and the results are given in Fig. 9. The photoproduction of H_2O_2 is in agreement with the photodegradation of OX, which proves that HO^\bullet produced from photocatalysis is the key to leading the degradation of CBZ. Similarly, two stages are observed by Seraghni et al. [20], at the initial stage where H_2O_2 was rapidly generated and the degradation of Cresol red (CR) was slow. However, at the later acceleration stage, when

Table 4

Abatement of acids and H₂O₂ formation as function of different concentration of acids during their photolysis upon irradiation at 365 nm

Acids	[acids] (M)	[H ₂ O ₂] _{max} · 10 ⁻⁵ (M)	Time (h)
SA	5.10 ⁻³	1.32	5
	10 ⁻³	1.29	6
	5.10 ⁻⁴	–	5
BE	5.10 ⁻³	3.36	7
	10 ⁻³	–	6
	2.10 ⁻⁴	–	6
MA	5.10 ⁻³	2.08	6
	10 ⁻³	1.88	–
OX	7.10 ⁻³	19.2	5
	5.10 ⁻³	22.3	5
	10 ⁻³	6.5	5
IDA	5.10 ⁻³	–	6

Table 5

Formation of H₂O₂ during the photolysis of OX at different light source

Wavelength (nm)	Acids	SA	BE	MA	OX	IDA
		[H ₂ O ₂] _{max} · 10 ⁻⁵ (M)	17	6.46	9.05	15.7
254	Time (min)	5	6	6	4	1
	[H ₂ O ₂] _{max} · 10 ⁻⁵ (M)	1.32	2.2	2.08	22.3	–
365	Time (min)	5	6	6	5	6
	[H ₂ O ₂] _{max} · 10 ⁻⁵ (M)	3.58	2.26	1.5	11.1	5.28
Solar light	Time (h)	1	5	1	1/6	1

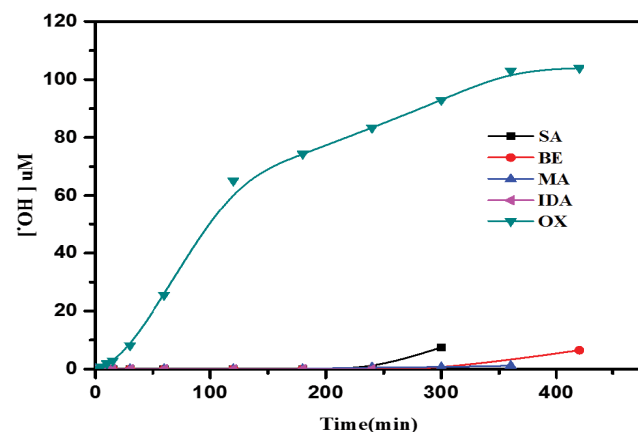


Fig. 7. Formation of •OH during the photolysis of different acids upon irradiation at 365 nm as a function of irradiation time, [acids] = 5 mM.

the concentration of H₂O₂ kept constant in this system, CR began to degrade at a high speed.

The influence of carboxylic acid nature was also studied and confirmed that the OX acid was the best photoinducer is reported in Fig. 9.

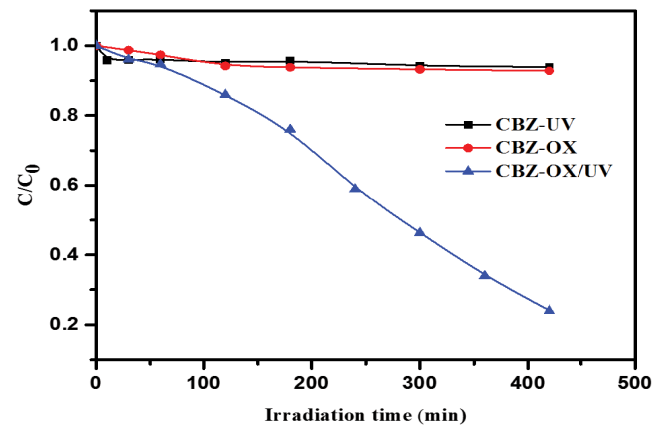


Fig. 8. Photodegradation of CBZ in the mixture CBZ-OX acid (0.01 mM and 5 mM) as a function of the irradiation time, λ_{irr} = 365 nm.

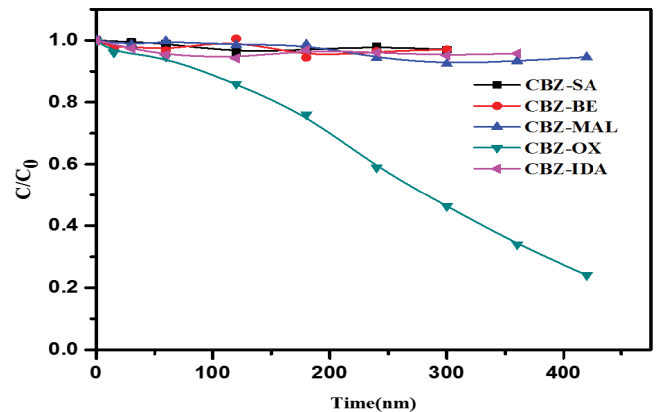


Fig. 9. Photodegradation of CBZ in the mixture CBZ-acids (0.01 mM and 5 mM) as a function of the irradiation time, λ_{irr} = 365 nm.

3.5. Mineralization of CBZ/OX/UVA

The mineralization of OX/CBZ was monitored measuring the total organic carbon (TOC), after 14 h of irradiation ca. 80% of TOC removal was observed. Incomplete mineralization was attributed to refractory photoproducts that would need a more prolonged treatment or that have already reached their maximum degree of oxidation (Fig. 10).

3.6. Environmental significance

In order to verify the feasibility of this system in a natural environmental, the system (CBZ 0.01 mM/OX acid 5 mM) was also tested under typical environmental irradiation conditions to confirm the viability of the process, exposed in natural light during a sunny day at Constantine (Algeria, latitude 36°22'N, longitude 6°40'E).

By comparing the kinetics of CBZ disappearance at natural and artificial light (Fig. 11), it appears that the rate of degradation is faster upon solar irradiation because of the wide range of the solar spectrum (Fig. 12).

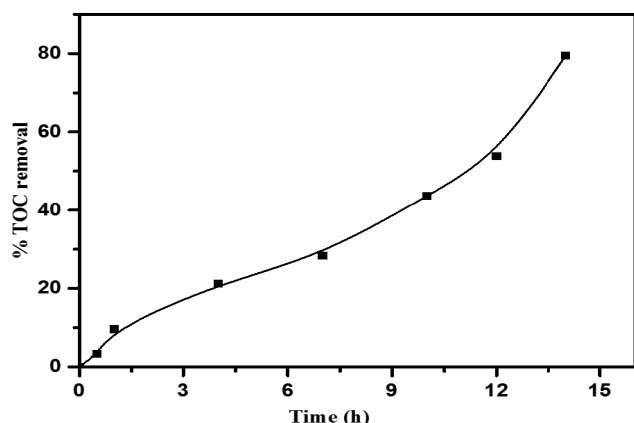


Fig. 10. Evaluation of TOC with time for the degradation of CBZ upon 365 nm irradiation. $[CBZ]_0 = 0.01$ mM and $[OX] = 5$ mM.

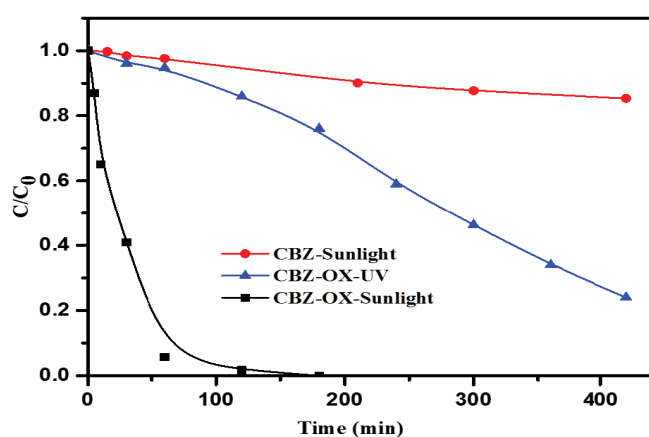


Fig. 11. Photodegradation of CBZ induced by OX (0.01 mM and 5 mM) during natural and artificial irradiation.

In natural conditions, a fast reaction was observed and the pollutant take less than 60 min to be completely removed. The solar spectrum contains several wavelengths explains this fact.

4. Conclusion

The organic acids confirm their viability to produce hydrogen peroxide when are exposed to irradiation up to 365 nm. This process was largely related to an organic acid structure where the oxalic acid used in this study was the most efficient. As H_2O_2 is generated by the reaction of $O_2^{\cdot-}$ and HO_2^{\cdot} , their quantification was an important element in understanding the mechanism of action of these species. This process seems to be dependent significantly on various factors including the initial pH value, the light source of irradiation and the acid concentration. The degradation efficiency of CBZ in the presence of oxalic acid (OX) is highly improved compared to other acids. The best formation of H_2O_2 and HO^{\cdot} is in perfect correlation with this fact.

Acknowledgments

We would like to thank the laboratory members who contributed to this work.

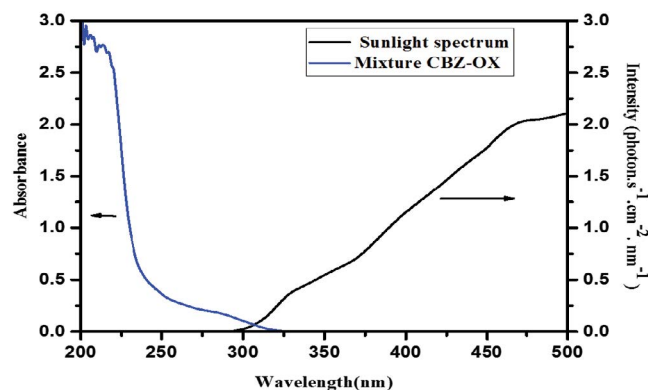


Fig. 12. Sunlight irradiance overlap with CBZ/OX UV-Vis absorption spectra. $[CBZ]_0 = 0.01$ mM and $[OX]_0 = 5$ mM.

Declaration of interests

The authors declare that they have no known competing financial interests or personal relationships that could have appeared to influence the work reported in this paper.

References

- [1] E.M. Thurman, Organic Geochemistry of Natural Waters, Springer Science & Business Media, Zotero Program, 2012.
- [2] E.M. Perdue, E.T. Gjessing, W. Glaze, Organic Acids in Aquatic Ecosystems, Wiley, Zotero Program, 1990.
- [3] A. Chebbi, P. Carlier, Carboxylic acids in the troposphere, occurrence, sources, and sinks: a review, Atmos. Environ., 30 (1996) 4233–4249.
- [4] R.W. Talbot, K.M. Beecher, R.C. Harriss, W.R. Cofer III, Atmospheric geochemistry of formic and acetic acids at a mid-latitude temperate site, J. Geophys. Res.: Atmos., 93 (1988) 1638–1652.
- [5] D.A. Hegg, S. Gao, H. Jonsson, Measurements of selected dicarboxylic acids in marine cloud water, Atmos. Res., 62 (2002) 1–10.
- [6] W.C. Keene, J.N. Galloway, J. David Holden Jr., Measurement of weak organic acidity in precipitation from remote areas of the world, J. Geophys. Res. C: Oceans, 88 (1983) 5122–5130.
- [7] M. Löflund, A. Kasper-Giebl, B. Schuster, H. Giebl, R. Hitznerberger, H. Puxbaum, Formic, acetic, oxalic, malonic and succinic acid concentrations and their contribution to organic carbon in cloud water, Atmos. Environ., 36 (2002) 1553–1558.
- [8] H.A. Khwaja, S. Brudnoy, L. Husain, Chemical characterization of three summer cloud episodes at Whiteface Mountain, Chemosphere, 31 (1995) 3357–3381.
- [9] S. Bikkina, K. Kawamura, Y. Miyazaki, P. Fu, High abundances of oxalic, azelaic, and glyoxylic acids and methylglyoxal in the open ocean with high biological activity: implication for secondary OA formation from isoprene, Geophys. Res. Lett., 41 (2014) 3649–3657.
- [10] R. Sempéré, K. Kawamura, Trans-hemispheric contribution of C2–C10 α , ω -dicarboxylic acids, and related polar compounds to water-soluble organic carbon in the western Pacific aerosols in relation to photochemical oxidation reactions, Global Biogeochem. Cycles, 17 (2003) 1069, doi: 10.1029/2002GB001980.
- [11] Y. Kamaya, Y. Fukaya, K. Suzuki, Acute toxicity of benzoic acids to the crustacean *Daphnia magna*, Chemosphere, 59 (2005) 255–261.
- [12] E.M. Thurman, Organic Geochemistry of Natural Waters, Zotero Program, 1985.
- [13] I.P. Pozdnyakov, V.F. Plyusnin, V.P. Grivin, E. Oliveros, Photochemistry of Fe(III) complexes with salicylic acid derivatives in aqueous solutions, J. Photochem. Photobiol., A, 307–308 (2015) 9–15.

- [14] H. Herrmann, B. Ervens, H.-W. Jacobi, R. Wolke, P. Nowacki, R. Zellner, CAPRAM2.3: a chemical aqueous phase radical mechanism for tropospheric chemistry, *J. Atmos. Chem.*, 36 (2000) 231–284.
- [15] M.R.A. Silva, A.G. Trovó, R.F.P. Nogueira, Degradation of the herbicide tebuthiuron using solar photo-Fenton process and ferric citrate complex at circumneutral pH, *J. Photochem. Photobiol., A*, 191 (2007) 187–192.
- [16] K. Kuma, S. Nakabayashi, K. Matsunaga, Photoreduction of Fe(III) by hydroxycarboxylic acids in seawater, *Water Res.*, 29 (1995) 1559–1569.
- [17] T. Zhou, X. Lu, J. Wang, F.-S. Wong, Y. Li, Rapid decolorization and mineralization of simulated textile wastewater in a heterogeneous Fenton like system with/without external energy, *J. Hazard. Mater.*, 165 (2009) 193–199.
- [18] C.Y. Kwan, W. Chu, The role of organic ligands in ferrous-induced photochemical degradation of 2,4-dichlorophenoxyacetic acid, *Chemosphere*, 67 (2007) 1601–1611.
- [19] B.H.J. Bielski, D.E. Cabelli, R.L. Arudi, A.B. Ross, Reactivity of HO_2/O_2^- radicals in aqueous solution, *J. Phys. Chem. Ref. Data*, 14 (1985) 1041–1100.
- [20] N. Seraghni, I. Ghoul, I. Lemmize, A. Reguig, N. Debbache, T. Sehili, Use of oxalic acid as inducer in photocatalytic oxidation of Cresol red in aqueous solution under natural and artificial light, *Environ. Technol.*, 39 (2018) 2908–2915.
- [21] J. Guo, Y. Du, Y. Lan, J. Mao, Photodegradation mechanism and kinetics of methyl orange catalyzed by Fe(III) and citric acid, *J. Hazard. Mater.*, 186 (2011) 2083–2088.
- [22] X. Ou, Y. Su, F. Zhang, C. Wang, Y. Wu, Photooxidation of Orange G in Aqueous Solution Induced by Irradiation of Fe(III)-Citrate Complex, 2011 International Conference on Remote Sensing, Environment and Transportation Engineering, IEEE, Nanjing, China, 2011, pp. 3319–3322.
- [23] X. Ou, X. Quan, S. Chen, F. Zhang, Y. Zhao, Photocatalytic reaction by Fe(III)-citrate complex and its effect on the photodegradation of atrazine in aqueous solution, *J. Photochem. Photobiol., A*, 197 (2008) 382–388.
- [24] I. Ghoul, N. Debbache, B.A. Dekkiche, N. Seraghni, T. Sehili, Z. Marin, J.A. Santaballa, M.C. López, Fe(III)-citrate enhanced sunlight-driven photocatalysis of aqueous carbamazepine, *J. Photochem. Photobiol., A*, 378 (2019) 147–155.
- [25] B.A. Dekkiche, N. Seraghni, N. Debbache, I. Ghoul, T. Sehili, Effect of natural and artificial light on Fe(III) organic complexes photolysis: case of Fe(III)-malonate and Fe(III)-malate, *Int. J. Chem. Reactor Eng.*, 17 (2018), doi: 10.1515/ijcre-2018-0106.
- [26] A. Safarzadeh-Amiri, J.R. Bolton, S.R. Cater, Ferrioxalate-mediated photodegradation of organic pollutants in contaminated water, *Water Res.*, 31 (1997) 787–798.
- [27] F.J. Millero, S. Sotolongo, The oxidation of Fe(II) with H_2O_2 in seawater, *Geochim. Cosmochim. Acta*, 53 (1989) 1867–1873.
- [28] B.C. Faust, R.G. Zepp, Photochemistry of aqueous iron(III)-polycarboxylate complexes: roles in the chemistry of atmospheric and surface waters, *Environ. Sci. Technol.*, 27 (1993) 2517–2522.
- [29] M. Fukushima, K. Tatsumi, Photocatalytic reaction by iron(III)-humate complex and its effect on the removal of organic pollutant, *Toxicol. Environ. Chem.*, 73 (1999) 103–116.
- [30] Y. Mameri, N. Debbache, M. El Mehdi Benacherine, N. Seraghni, T. Sehili, Heterogeneous photochemical degradation of paracetamol using goethite/ H_2O_2 and goethite/oxalic acid systems under artificial and natural light, *J. Photochem. Photobiol., A*, 315 (2016) 129–137.
- [31] M. El Mehdi Benacherine, N. Debbache, I. Ghoul, Y. Mameri, Heterogeneous photoinduced degradation of amoxicillin by goethite under artificial and natural irradiation, *J. Photochem. Photobiol., A*, 335 (2017) 70–77.
- [32] A. Durán, J.M. Monteagudo, A.J. Expósito, V. Monsalve, Modeling the sonophoto- degradation/mineralization of carbamazepine in aqueous solution, *Chem. Eng. J.*, 284 (2016) 503–512.
- [33] A. Ghauch, H. Baydoun, P. Dermesropian, Degradation of aqueous carbamazepine in ultrasonic/ $\text{Fe}^0/\text{H}_2\text{O}_2$ systems, *Chem. Eng. J.*, 172 (2011) 18–27.
- [34] J.-K. Im, H.-S. Son, Y.-M. Kang, K.-D. Zoh, Carbamazepine degradation by photolysis and titanium dioxide photocatalysis, *Water Environ. Res.*, 84 (2012) 554–561.
- [35] J. Deng, Y. Shao, N.-Y. Gao, Y. Deng, S. Zhou, X. Hu, Thermally activated persulfate (TAP) oxidation of antiepileptic drug carbamazepine in water, *Chem. Eng. J.*, 228 (2013) 765–771.
- [36] G. Eisenberg, Colorimetric determination of hydrogen peroxide, *Ind. Eng. Chem. Anal. Ed.*, 15 (1943) 327–328.
- [37] R.H. Schuler, G. Albarran, The rate constants for reaction of OH radicals with benzene and toluene, *Radiat. Phys. Chem.*, 64 (2002) 189–195.
- [38] J. Guo, J. Zhang, C. Chen, Y. Lan, Rapid photodegradation of methyl orange by oxalic acid assisted with cathode material of lithium ion batteries LiFePO_4 , *J. Taiwan Inst. Chem. Eng.*, 62 (2016) 187–191.
- [39] E.M. Rodríguez, B. Núñez, G. Fernández, F.J. Beltrán, Effects of some carboxylic acids on the Fe(III)/UVA photocatalytic oxidation of muconic acid in water, *Appl. Catal., B*, 89 (2009) 214–222.
- [40] E.M. Rodríguez, G. Fernández, N. Klammerth, M.I. Maldonado, P.M. Álvarez, S. Malato, Efficiency of different solar advanced oxidation processes on the oxidation of bisphenol A in water, *Appl. Catal., B*, 95 (2010) 228–237.